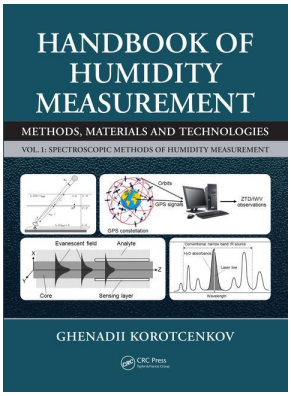

Handbook of Humidity Measurement
Methods, Materials and Technologies: Spectroscopic Methods of Humidity Measurement

Ghenadii Korotcenkov

Upper Tropospheric and Stratospheric Water Vapor Control

Publication details
https://test.routledgehandbooks.com/doi/10.1201/b22369-9
Ghenadii Korotcenkov
Published online on: 26 Mar 2018

9 Upper Tropospheric and Stratospheric Water Vapor Control

9.1 THE ROLE OF WATER VAPORS IN THE UPPER TROPOSPHERE AND LOWER STRATOSPHERE

As it was indicated in Section 2.8, the water vapor distribution in the upper troposphere (UT) and lower stratosphere (LS) is of central importance in several ways (Kley et al. 2000): it plays a major role in the balance of planetary radiation; it influences and responds to atmospheric motions; and it plays a key role in many aspects of UT/LS chemistry. Effects on the radiation balance are especially important because the water vapor molecule is strongly polar in shape giving it a strongly absorbing infrared (IR) spectrum. Water vapor is the dominant atmospheric greenhouse gas, and because the amount of water vapor which can be held by the atmosphere increases strongly with temperature, it is very sensitive to changes in climate. For example, the inclusion of water vapor and other climate feedbacks within general circulation models (GCMs) produces ~3°C of warming for a doubling of CO_2 from preindustrial times, compared to 1.2°C of warming calculated without feedbacks (IPCC 2007). Thus, it is clear that changes in the water vapor concentration have important significance for the formation of the Earth's climate.

Although water vapor in the stratosphere is present at levels much lower than those in the troposphere, these very changes in stratospheric water vapor have a profound impact on radiative forcing and surface temperatures. It was established that longwave radiation at the wavelengths of water absorption is fully attenuated in the lower troposphere, such that increasing water vapor concentrations at those levels will have no impact on radiative forcing. However, surface temperatures are very sensitive to changes in water vapor in the UT and LS, where water vapor absorption lines are unsaturated. De F. Forster and Shine (1999), extending earlier work of Rind and Lonergan (1995), calculated that if the increase in the lower stratospheric H_2O mixing ratio reported over Boulder, Colorado, from 1979 to present, by Oltmans and Hofmann (1995) is occurring globally, the contribution to surface warming would be 40% of that from the CO_2 increase over the same time period. Solomon et al. (2010) determined that a 1 ppmv increase (~1% per year) in stratospheric water vapor between 1980 and 2000, though uncertain, would have enhanced the rate of surface warming over that period by ~30% compared to estimate without this change. The 0.4 ppmv decrease in water vapor after 2001 acted to reduce the rate of global surface warming from 2000–2009 by ~25%. The combination of these trends likely contributed to the observed flattening of the global surface warming trend observed in the past decade. De F. Forster and Shine (1999) also emphasized that an increase of water vapor causes a cooling of the LS that is comparable to the contribution due to ozone changes.

It was found that the increased stratospheric water vapor levels could also enhance ozone destruction. Water vapor is a source of HO_x radicals in the stratosphere, which catalytically destroy ozone. At the poles, elevated water vapor also increases the formation and persistence of polar stratospheric clouds (PSCs); a 1 ppmv increase in water vapor increases the threshold temperature for PSC activation by ~1°C, which would increase the spatial and temporal extent of polar ozone loss (Kirk-Davidoff et al. 1999). Elevated water vapor also increases activation of sulfate-water aerosols for ozone depletion, both at the poles and at middle attitudes. Deep convective outflow has been observed to produce plumes with up to 12 ppmv of water vapor in the middle attitude stratosphere, which could potentially activate halogen-catalyzed ozone loss on sulfate-water aerosols, leading to destruction of up to 25% of local ozone more than seven days (Anderson et al. 2012). Deep convection can also transport very short-lived bromine and iodine species into the stratosphere on short timescales, which would amplify this ozone destruction. If increasing global surface temperatures lead to a greater frequency of such deep convective events, substantial local ozone destruction could be observed

in the summer over populated areas. This means that the increase in the stratospheric concentration of water vapor presents a continuing threat to the global ozone layer.

Increased climate forcing by greenhouse gases is also predicted to increase continental convective activity at middle attitudes. In particular, climate models show that increased atmospheric moisture content in a warmer climate leads to an increase in the frequency and intensity of severe storms over the United States (Trapp et al. 2009; Van Klooster and Roebber 2009). Such changes could increase the amount of ice transported into the stratosphere by convection, increasing water vapor in both the lowermost stratosphere and overworld. As the lowermost stratosphere is a region of descent, increases in water vapor there would have an important local radiative impact, but would not impact the global stratosphere. However, elevated water vapor above the 380 K isentrope could be isentropically transported into the tropics where it would enter the mean circulation and moisten the overworld stratosphere while bypassing the cold point (Dessler and Sherwood 2004).

It is therefore critical to better understand how stratospheric water vapor will be affected by a changing climate to predict future changes and their feedback on the climate system. The climate feedbacks of tropospheric water vapor are well represented in climate models because water vapor at these levels closely follows temperature changes. On the other hand, the processes that control water vapor in the stratosphere are not well understood, which makes predictions of stratospheric water vapor levels and their radiative feedbacks much more uncertain. From the results presented by Harries (1997), one can realize that it is very important to have reliable information about the state of the atmosphere. Harries (1997) pointed out that, because the effects of water vapor on the Earth radiative balance are so large, small errors in spectroscopic parameters and in radiative-dynamical models used to model the energy balance, can produce potentially large uncertainties in the prediction of climatic change. He presented evidence from sensitivity studies showing that the humidity concentration, particularly in the UT may need to be known with accuracy in the range of 3%–10% to avoid uncertainties in calculated radiative forcing that are of the order of the effect due to doubling CO_2 concentrations.

These facts emphasize the urgent need to understand the behavior and to assess the concentration of the water vapor in the UT and LS, to detect short- and long-term trends in stratospheric water vapor, and to establish the mechanisms, which control upper tropospheric and stratospheric humidity.

9.2 WATER VAPOR MONITORING IN TROPOSPHERE AND STRATOSPHERE

The previous analysis has shown that atmospheric water vapor is abundant in the atmosphere and possesses absorption features spread over a broad range of the electromagnetic spectrum. Therefore, it should be easy to measure the concentration of water vapor in UT and stratosphere. However, in practice, water vapor measurements in these areas have proved to be difficult. Water sticks to surfaces, thereby providing challenges for *in situ* techniques. Sharp vertical and horizontal gradients present difficulties for remote sensing techniques. A lack of understanding of the fundamental physics behind the observed spectrum complicates the analysis of remote sensing measurements. The radiative effects of clouds are yet another complicating factor in making water vapor measurements. In addition, comparisons between satellite and direct water vapor measurements from *in situ* observations present a difficulty. This was due mainly to problems with the *in situ* methods, especially the radiosondes, and also because of difficulties in making comparisons in an inhomogeneous atmosphere when instruments have very different spatial coverage and altitude resolution. As a result, our understanding of the distribution of upper tropospheric and lower stratospheric water vapor is not as thorough as it should be.

As follows from Chapters 4 through 8, the study of UT and stratosphere can be carried out using either a remote sensing instruments, installed at ground stations, or *in situ* monitoring using instruments mounted on balloons (Figure 9.1a), satellites (Figure 9.1b), and aircrafts (Kley et al. 2000; Pankine et al. 2009). The advantage of most *in situ* techniques is their higher precision and spatial resolution compared to remote sensing instruments; thus *in situ* instruments are well suited particularly for case studies on smaller scales. Their absolute calibration either in the laboratory or in flight, tracing to calibration standards can be repeated at regular intervals and possible instrument drifts are easier to detect. There is no need for additional algorithms for the measurement geometry. At the same time, the retrieval of atmospheric water vapor profiles from ground-based measurements is a difficult task due to its large vertical gradient and large temporal variability; and standard retrieval methods are often not

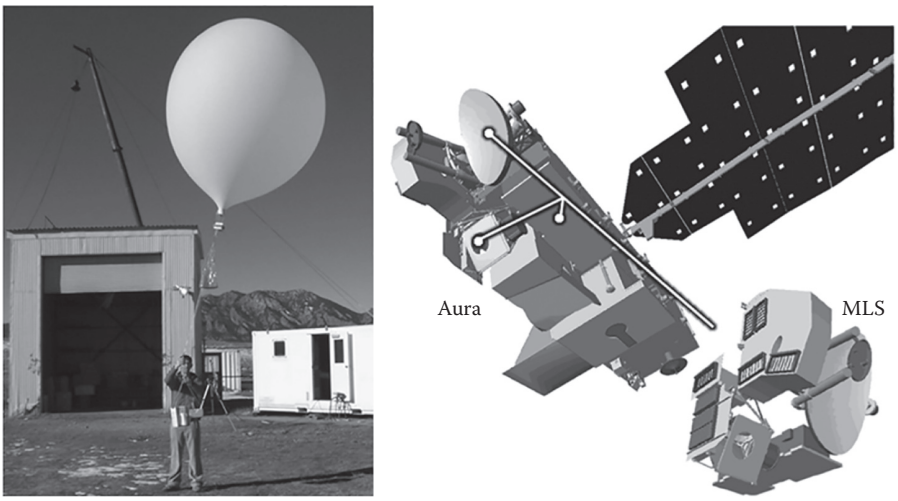

(a) (b)

FIGURE 9.1 (a) Launching of a balloon for meteorological observations (From http://www.esrl.noaa.gov/gmd/ozwv/wvap/) and (b) Satellite with AURA-Microwave Limb Sounder (MLS) (From http://www.mls.jpl.nasa.gov/). The Earth Observing System (EOS) MLS is one of four instruments on the NASA's EOS Aura satellite, launched on July 15, 2004. MLS makes measurements of atmospheric composition, temperature, humidity, and cloud ice. The MLS measurements are made globally day and night. A feature of the MLS technique is that its measurements can be obtained in the presence of ice clouds and aerosol that prevent measurements by shorter-wavelength infrared, visible, and ultraviolet techniques. The EOS MLS measures thermal emission from broad spectral bands centered near 118, 190, 240, 640, and 2500 GHz are measured continuously (24 h per day) by 7 microwave receivers (2 each at 118 and 2500 GHz) using a limb viewing geometry, which maximizes signal intensities and vertical resolution. MLS is radiometrically calibrated after each 25 s limb scan. The EOS MLS instrument contains three modules: (1) The GHz radiometer module, which includes the 118–640 GHz receivers and a scanning offset antenna with 0.8 × 1.6 m primary mirror; (2) The THz radiometer module which contains the 2500 GHz receivers and the THz telescope and scan mirror, whose scan is synchronized with that of the GHz antenna; and (3) The Spectrometer module which receives signals from the GHz and THz radiometer modules, detects and digitizes them, and passes the digitized signals to the spacecraft for telemetry to the ground.

suited (Schneider et al. 2013). The development of water vapor retrievals has recently made substantial progress, but still no common water vapor retrieval method is applied at all NDACC sites. *In situ* instruments are therefore often used for the validation of space-borne remote sensing experiments. Since the operation of *in situ* instruments in the UT/LS requires the use of platforms such as balloons or aircraft, which are either expensive to operate, have limited availability, or both, the data sets cover only limited regions and time periods. This disadvantage is partly compensated by the large number of measurements made to date.

With regard to the comparison of opportunities for research using balloons and aircrafts, it should be noted that these studies tend to solve various tasks. Of course, more complicated equipment, which can allow conducting more complex experiments can be installed at aircrafts. The ability of the aircraft to go when and where observations are needed makes it also very valuable for atmosphere monitoring. Moreover, it is possible with long range jet aircraft to reach any spot on the globe. This means that it is able to cover a large geographical range with a number of flights. In addition, jet aircraft can reach the UT or LS depending on the latitude, and thus, are above most of the water vapor that prevents observation from the ground at many wavelengths. However, the number of aircrafts that can be used for research is very limited. In addition, the use of aircraft has weather restrictions. Another disadvantage of using aircrafts as observing platforms is their inability to reach the altitudes of greatest interest for stratospheric chemistry. The vibration level which can cause noise problems is also a shortcoming of aircraft platform.

Regarding satellite possibilities for controlling the water vapor distribution in the atmosphere, then of course they are used (Noël et al. 1999; Sherwood et al. 2010). But of course, these measurements may not be *in situ* measurements. Weather satellites are operated

by agencies in China, France, India, Japan, Korea, the Russian Federation, the United States and Eumetsat for Europe, with international coordination by the World Meteorological Organization (WMO). In addition to geostationary weather satellites around 160 environmental satellite missions in low-earth orbit are currently measuring selected climate parameters. As a rule, for remote monitoring of water vapor in the atmosphere satellites equipped with microwave radiometers (Engelen and Stephens 1999; Susskind et al. 2003; Froidevaux et al. 2006; Waters et al. 2006) or with multichannel spectrometers (Schmetz et al. 2002; Buehler et al. 2008; Fetzer et al. 2008; Chou et al. 2009) (Table 9.1). For example, the Atmospheric Infrared Sounder (AIRS) contains hundreds of channels in the water vapor absorption bands and can resolve vertical layers of a few kilometers. However, even this sounder is still affected by cloud cover and tends to underestimate wet and dry relative humidity extremes (Fetzer et al. 2008; Chou et al. 2009). As it was shown in Chapter 5, the microwave radiation is less affected by clouds and thus offers a useful alternative method of moisture sounding from space. In particular, advanced microwave sounding unit (AMSU) is able to detect humidity averaged over several broad layers, especially in the UT, with significant interference only from thick clouds (Engelen and Stephens 1999; Susskind et al. 2003). Similar instruments that observe limb emission, the two Microwave Limb Sounders (MLSs, first flown in 1991), observe moisture above ~350 hPa (Froidevaux et al. 2006; Waters et al. 2006). We should also not forget possibilities of the global positioning system (GPS) technology, considered in Chapter 6. This technology can be used to estimate a total column water vapor over suitably equipped surface stations (Wang and Zhang 2008). The GPS technique has the important advantages of being an absolute measurement that does not need an independent

TABLE 9.1
Estimates of Random Errors, Systematic Errors and Vertical Resolution of Stratospheric H_2O Profiles Derived from Satellite Instrumentation

Instrument and Data Set	Random Error	Systematic Error	Vertical Resolution, km
LIMS (version 5)	20–15% (1–5 hPa)	31–24% (1–5 hPa)	~5
(Limb IR emission)	15–10% (5–10 hPa)	24–20% (5–10 hPa)	
	10% (10–50 hPa)	20–37% (10–50 hPa)	
SAGE II (version 5.9)	10–5% (3–10 hPa)	6–13% (3–7 hPa)	~3
(IR solar occultation)	5–14% (10–25 hPa)	13% (7–25 hPa)	
	14% (25–300 hPa)	13–27% (25–100 hPa)	
		27% (100–300 hPa)	
ATMOS (version 3)	9–11% (1–300 hPa)	6% (1–300 hPa)	3–6
(IR solar occultation)			
HALOE (version 19)	9–7% (1–10 hPa)	10–14% (1–10 hPa)	2.3
(IR solar occultation)	7–13% (10–40 hPa)	14–19% (10–40 hPa)	
	13% (40–100 hPa)	19–24% (40–100 hPa)	
MLS (version 0104)	4% (1–10 hPa)	6–9% (1–10 hPa)	~3
(Limb microwave emission)	3% (10–50 hPa)	9–16% (10–50 hPa)	
	3–8% (50–100 hPa)	16–50% (50–100 hPa)	
MAS (Limb microwave emission)	5–10% (1–50 hPa)	10–15% (1–50 hPa)	~5
ILAS (version 4.20)	More than 10% above 2 hPa	30% (1–2 hPa)	1–2
(IR Solar occultation)	10–5% (2–300 hPa)	30–10% (2–7 hPa)	
		10% (7–300 hPa)	
POAM III (version 2)	5% (3–100 hPa)	15% (3–100 hPa)	1–3
(IR solar occultation)			

Source: Kley D. et al., SPARC Report No. 2. World Climate Research Programme, Geneva, Switzerland, 2000.
ATMOS—Atmospheric Trace Molecule Spectroscopy, ILAS—Improved Limb Absorption Spectrometer, LIMS—Limb Infrared Monitor of the Stratosphere, MAS—Microwave Atmospheric Sounder, MLS—Microwave Limb Sounder (on UARS), POAM—Polar Ozone and Aerosol Measurements, SAGE—Stratospheric Aerosol and Gas Experiment.

calibration and of not being affected at all by clouds or other absorbers (although temperature must be known fairly well to achieve good accuracy).

9.3 PECULIARITIES OF AIRCRAFT OBSERVATIONS—FACTORS INFLUENCING THE IN-FLIGHT PERFORMANCE

Experiments have shown that numerous factors can influence the in-flight performance of airborne water vapor measurements. In particular, of crucial importance are the sticking of water vapor at surfaces and the appropriate use of sampling systems (Kley et al. 2000; Bange et al. 2013).

Water molecules are highly polar, such that water molecules attach themselves tenaciously to surfaces. Particularly, at low temperatures, this can lead to large memory effects of the water vapor measurements. Additional heating may eliminate any such memory effects. Therefore, the selection of hygrophobic materials is an important part of the sampling and measuring systems design of the hygrometer. In general, to avoid any water vapor contamination or memory effect from the aircraft skin, it is most favorable that the air inlets are sampling air outside the aerodynamic boundary layer at the aircraft skin. In addition, moisture must not be allowed to leak into the measurement system or interface with the measurements. This is the most critical in dry regions or at low humidities in the UT and stratosphere. Therefore, most airborne hygrometers use extractive sampling systems that force the samples ambient air through an appropriate inlet system into a closed-path detector system installed inside the aircraft. Usually the sideward or backward facing type of air inlets are deployed by using a pump, and the forward directed type of air inlets use the ram pressure caused the moving aircraft, such as fast Lyman–alpha or IR absorption hygrometers, or open-path TLAS systems. These open-path systems have the advantages of virtually eliminating contamination. The heating of the instrument and its inlet before measurements can also be used for decrease of contamination influence.

It should be noted that similar problems exist in the measurements carried out with the use of balloons. Therefore, proper selection of wall materials, optimization of probe location (increasing the distance between a measurement unit and balloon), heating of the instrument and its inlet, large flow rates, or open-cell designs have to be used to avoid or minimize measurement artifacts (Kley et al. 2000).

9.4 COMPARATIVE CHARACTERISTICS OF THE DEVICES USED FOR THE UPPER TROPOSPHERIC AND STRATOSPHERIC MEASUREMENTS

Tropospheric and stratospheric water vapor has been measured more than the past 50 years by a large number of individuals and institutions using a variety of *in situ* and remote-sensing measurement techniques (Mastenbrook 1968; Bertaux and Delannoy 1978; Kley and Stone 1978; Kley et al. 1979; Buck 1985; Goutail and Pommereau 1987; Vömel et al. 2007; Leblanc et al. 2012; Hurst et al. 2011, 2014). Operating principles and measurement specifications of most *in situ* research-type instruments currently in use are presented in Table 9.2 along with their estimated measurement accuracy. These instruments provide point measurements in time and space with high vertical resolution, typically in the range of a few hundred meters or better. Accuracy estimates range from 5% to 10% based on known or estimated random and systematic uncertainties inherent in the instrument system, calibration procedures and retrieval

TABLE 9.2
***In Situ* and Remote-Sensing Techniques for Measurements of H_2O from Ground-Based, Balloon-Borne and Airborne Platforms, along with Their Typical Measurement Range and Overall Accuracy, That Is, the Sum of Systematic and Random Errors**

Technique	Range	Altitude Range	Accuracy
Lyman–alpha fluorescence	500–0.2 ppmv	5–35 km	6–7%
Tunable diode laser spectrometry	>0.1 ppmv	0–30 km	5–10%
Microwave spectrometry	20–0.2 ppmv	20–80 km	0.6–0.2 ppmv
LIDAR	>4 ppmv	0–20 km	5–10%
IR and FTIR spectrometry	>1 ppmv	5–40 km	5–13%
Frost point hygrometry	10,000–0.5 ppmv	5–30 km	5–10%
MOZAIC sensor	>20 ppmv	Troposphere	5–7% RH
Radiosonde	100 ≈ 5% RH	Middle and lower troposphere	not assessed

Source: Kley D. et al., SPARC Report No. 2. World Climate Research Programme, Geneva, Switzerland, 2000.

FIGURE 9.2 LIDAR system designed by Jet Propulsion Laboratory (JPL) Table Mountain Facility (TMF) atmospheric LIDAR group. (From http://www.tmf.jpl.nasa.gov/tmf-lidar/.)

algorithms. Remote sensing instruments deployed on ground-based (Figure 9.2), balloon-borne and airborne platforms provide vertical profile measurements with stated accuracy similar to *in situ* instruments, although with coarser vertical resolution. Such vertical resolutions range from several hundred meters in the case of light detection and ranging (LIDAR), to a few kilometers for the IR and far-infrared (FIR) spectrometers, and approximately 10 km for microwave instruments.

A survey of different techniques designed for satellite application and their performance is presented in Table 9.1. The vertical resolution of satellite instruments depends on the individual measurement concept (e.g., occultation or emission) and the specific instrument implementation. Horizontal resolution is typically on the order of 50–300 km depending on whether the experiment is nadir or limb viewing.

Despite the significant research experience gained over the past decades, measurements of atmospheric humidity in upper tropospheric and stratospheric regions have been and continue to be a challenging task. Measurements of water vapor in the UT and in the stratosphere require tremendous technical effort due to the large gradients around the tropopause and the low stratospheric mixing ratios of a few ppmv in contrast to the moist tropospheric air masses. Further, in the stratosphere, the spatial and temporal variability of the H_2O abundance is relatively small, that is, changes of a few tenths of 1 ppmv need to be detected with a similar accuracy of the measurement. Therefore, till now there is no sensor available that can cover the full dynamic range of water vapor levels from a few percentages near the surface down to a few of ppmv in 15–20 km altitude. This means that there is no single existing instrument which is capable of H_2O measurements at all altitudes, with adequate global and temporal coverage. Figure 9.3 shows a diagram of the altitude range and platforms for the most important techniques. It is seen, while a broad

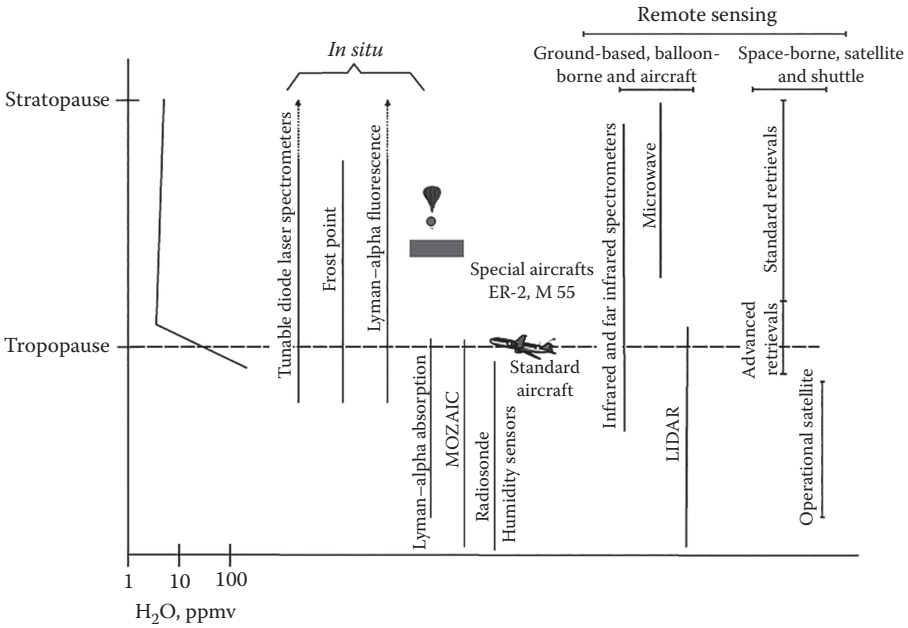

FIGURE 9.3 Typical vertical profile of water vapor in the upper troposphere and the stratosphere, the altitude range where the techniques described in this Assessment can be applied, and the carriers available for integration of the different instruments. (From Kley D. et al., SPARC Report No. 2. World Climate Research Programme, Geneva, Switzerland, 2000.)

spectrum of instruments exists today, all of them have their limitations (Beaton and Spowart 2012).

For example, the chilled-mirror hygrometer, commonly used for aircraft-based water vapor measurements, directly measures the dew point or frost point of the air. While these instruments are inexpensive, easy to deploy, and accurate, the need to adjust the temperature of the mirror makes them slow to respond, requiring seconds or even tens of seconds, and they often overshoot or oscillate when subjected to large, abrupt humidity changes.

Earlier in Chapters 3 and 4, it was shown that optical water vapor absorption-measuring methods are a powerful tool for monitoring the atmosphere. They are based on tunable diode lasers (May 1998; Zondlo et al. 2010), with data rates of 10–25 samples per second, equivalent to a bandwidth of 5–12.5 Hz (Shannon 1949). These instruments provide an independent absolute measurement of the water vapor number density in the troposphere and LS, but their using require very careful calibration, with consideration to the pressure, temperature, and homogeneous and heterogeneous broadening coefficients of water vapor. They also require skilled field support because troubleshooting and repair can be very difficult. Another limitation for the use of TDLAS hygrometers for these purposes is a significant shift in the central wavelength of absorption when the altitude is changed (Table 9.3). This means that the coordination of the laser radiation and the absorption spectrum by water vapor, required for this method, can be violated.

Nondispersive infrared (NDIR) instruments such as the LI-COR LI-7500 have also been deployed. This instrument has a bandwidth of up to 20 Hz; however, the large sample volume, roughly 30 cm^3 or larger, is designed for ground-based flux measurements and is not suitable for mounting outside an aircraft without significantly strengthening the optical assembly, even at airspeeds below 50 m/s (Hall et al. 2006). If mounted inside the aircraft, it requires a very large airflow to exchange the air inside the large sample volume at 20 times per second. For comparison, the Zeeman-split argon emission hygrometer described by Kebabian et al. (2002) has a sample volume of 300 cm^3, and they employed a 600 L/min flow to sufficiently clear the cell for measurements in a 10-Hz bandwidth.

Until recently, Lyman–alpha absorption hygrometers were the preferred high-rate hygrometers for water vapor measurements from research aircraft. These instruments were inexpensive, provided data with a bandwidth of 25 Hz, and required no optical alignment or skilled field support, only occasional cleaning of the lamp and detector windows. However, because of pressure- and temperature-dependent interference from atmospheric oxygen, and to a lesser extent carbon dioxide, which also absorbs at this wavelength, and drift in the electronics, lamp output, and detector responsivity, the Lyman–alpha hygrometer often was used as a high rate signal only, with the long-term output forced to follow that of a slower, more accurate sensor, such as the chilled-mirror dew point sensors by a loose-coupling algorithm such as described by Schanot (1987). There have been attempts to remove the oxygen interference through variable pathlength (Buck 1976), multiwavelength (Weinheimer and Schwiesow1992), and reference path techniques (Zuber and Witt 1987), but for a variety of reasons these have not been widely deployed on aircraft. Recent developments made in Harvard University (Cambridge, Massachusetts) (Hintsa et al. 1999) and in the National Center for Atmospheric Research (Boulder, Colorado) (Beaton and Spowart 2012) contributed to the improvement of parameters of Lyman–alpha absorption hygrometers. A schematic of the Harvard Water Vapor (HWV) instrument based on the Harvard Lyman–alpha hygrometer is shown in Figure 9.4. This instrument was designed for aircraft applications. However, the main disadvantages of Lyman–alpha absorption hygrometers, indicated earlier, still exist.

Similar hygrometers (Campbell and Tanner 1985) have been designed around krypton lamps, which have emission lines near the Lyman–alpha line—a strong emission line at 123.6 nm and a weaker line at 116.5 nm. While the krypton lamps are stable, long-lived, inexpensive sources, they are notably inferior from a spectroscopic standpoint. At 123.6 nm, the water vapor absorption strength is down by a factor of almost 2, whereas the oxygen absorption is stronger by a factor of about 40 (Tillman 1965; Yoshino et al. 1996), making the oxygen interference much more severe and variable

TABLE 9.3
Effect on the Altitude of the Measurement on the Position of Central Wavelength of Water Vapor Absorption

Central Wavelength of Absorption, μm	The Area of Measurement
7.43	Lower-tropospheric humidity
7.02	Mid-tropospheric humidity
6.51	Upper-tropospheric humidity

Source: Menzel, W.P. and Purdom, J.F.W., *Bull. Am. Meteo. Soc.*, 75, 757–781, 1994.

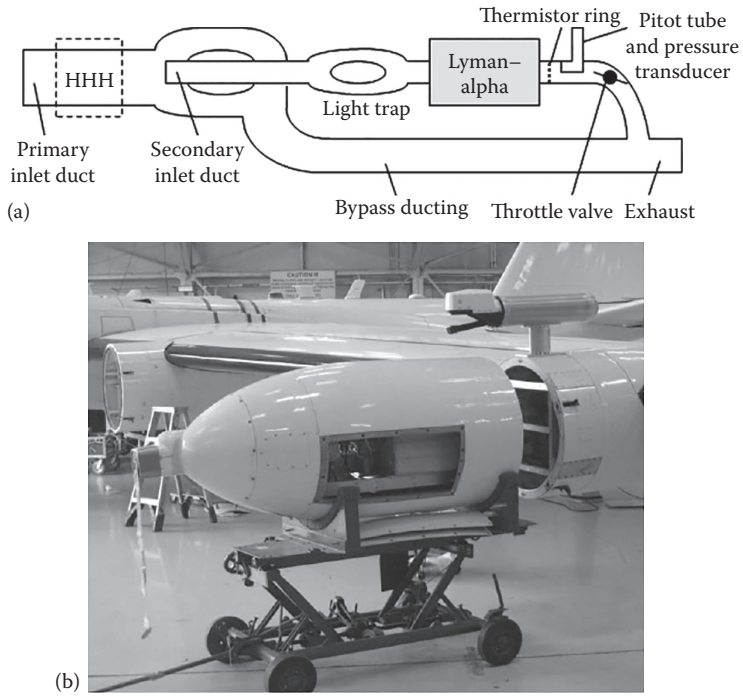

FIGURE 9.4 (a) A schematic of the HWV instrument. The Lyman–alpha detection axis and the subsystems that measure temperature and pressure and control the velocity through the instrument duct are labeled; the location of the HHH detection axis, which was included in the payload for the first time in the 2011 MACPEX campaign, is also indicated. Harvard Herriott Hygrometer (HHH) is an independent water vapor measurement. HHH uses a tunable diode laser (TDL) to measure water vapor via direct absorption in the infrared range. (b) The HWV instrument as it was flown in 2011 using a 3.5 × 4″ rectangular primary inlet which incorporates the HHH detection axis. (From http://www.nasa.gov.)

with air density, a particular problem for measurements from aircraft.

Thus, one can see that an ideal instrument capable of measuring the concentration of water vapor in all possible conditions does not exist. Moreover, one should recognize that there is no single technique or instrument platform that is recognized as a standard to which other techniques should be compared. This means that the development and operation of precise and accurate hygrometers for the atmosphere monitoring as well as their accurate calibration is still at the research level and is far from being routine. For example, in recent years there have been studies aimed at developing methods of water vapor measurements based on the use of airborne mass spectrometers (AIMS–H_2O). In particular, Kaufmann et al. (2016) presented a new setup based on linear quadrupole mass spectrometers (LQMS) to measure water vapor by direct ionization of ambient air (Figure 9.5). Air was sampled via a backward facing inlet that includes a bypass flow to assure short residence times (<0.2 s) in the inlet line, which allows the instrument to achieve a time resolution of ~4 Hz, limited by the sampling frequency of the mass spectrometer. From the main inlet flow, a smaller flow is extracted into the novel pressure controlled gas discharge ion source of the mass spectrometer. Developed instrument had possibility to quantify low water-vapor mixing ratios typical for the UT and LS with a high accuracy between 7% and 15% in the measurement range between 1 and 500 ppmv, depending on specific humidity and time resolution of the measurement. Of course, this powerful tool is not simple, cheap, and portable, which can be used for example, in the measurements carried out with the use of balloons. But its application can enhance the possibilities of scientific research in this field.

The same situation takes place when comparing methods, used for remote monitoring. For example, the comparison of the total precipitable water vapor (PWV) from air measured using FTIR spectroscopy with data, obtained by other methods, has shown the following (Schneider et al. 2009, 2010a, b): when it was compared with instruments such as a Multifilter Rotating Shadow-band Radiometer (MFRSR), a Cimel sun photometer, a GPS receiver, and daily radiosondes (Vaisala RS92), it was estimated that the FTIR spectrometer provides very precise trophospheric water vapor data, but when the area-wide coverage and real-time data availability is very important, the GPS and the RS92 data

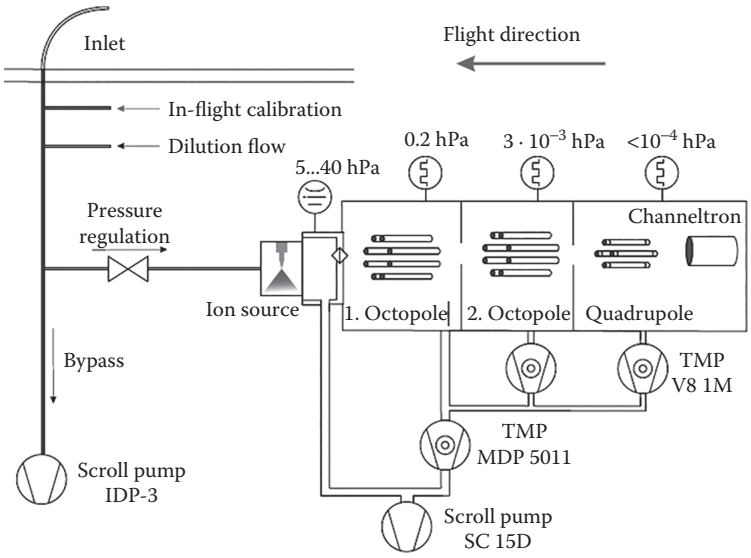

FIGURE 9.5 Schematic of the flight configuration of AIMS. Ambient air enters via a backward faced inlet and passes through a pressure regulation valve before entering the ion source. The ion beam is then focused by two adjacent octopoles and finally separated by mass-to-charge ratio in the quadrupole. In addition, connections for an optional dilution of ambient air and background measurements and for addition of trace gases for in-flight calibration are mounted right beneath the inlet. (From Kaufmann S. et al., *Atmos. Meas. Tech.* 9, 939, 2016. Published by the European Geoscience Union as open access.)

are more appropriate. At the same time, the FTIR spectroscopy can be used as a reference when assessing the accuracy of the other techniques, but those who use this technique have to be aware of the FTIR's significant clear sky bias.

Palm et al. (2010) also did comparisons between total water vapor column amounts measured by the ground-based FTIR, the ground-based microwave radiometer for atmospheric measurments (RAM), and by the satellite sensors Scanning Imaging Absorption Spectrometer for Atmospheric Chartography (SCIAMACHY) and Advanced Microwave Sounding Unit B (AMSU-B). It was shown that the microwave sensors, RAM and AMSU-B, operate best in winter, when the IWV is low. They are partly independent of weather conditions; that is, light clouds do not distort the measurements beyond recovery. The IR sensor, FTIR, depends on clear sight to the Sun, that is, no clouds between the instrument and the Sun. The optical sensors, SCIAMACHY and The Global Ozone Monitoring Experiment (GOME), also depend on solar light. Due to the short wavelength of the radiation recorded by the SCIAMACHY and the GOME instrument, clouds disturb the measurements considerably. This fact makes it necessary to cloud filter those measurements. The GPS IWV is derived from the zenith path delay (ZPD) standard product of the International GNSS Service (IGS) global network processing. It measures all year round and is independent of weather.

It was also established that measurements from ground-based remote sensors, Solar-FTIR and GPS (IWV higher than 10×10^{21} mol/cm^2), were of superior quality (Palm et al. 2010). The satellite instruments, AMSU-B, SCIAMACHY, and GOME, also performed well if errors are taken into account. For the AMSU-B measurements this included IWV higher than 30×10^{21} mol/cm^2. The higher variance of the satellite-based instruments may be explained by the spatial coverage and by the high variance of IWV. The Lunar-FTIR exhibited a low SNR and very sparse measurements necessitating long coincidence times to enable radiosonde comparisons. The Lunar absorption measurements using the FTIR are very sparse and also rather noisy. However, the Lunar-FTIR gives possibility to make measurements during the night. The measurements of the RAM were of fair quality. It has to be taken into account; however, that the RAM is not designed for measuring the IWV but this is a by-product of the O_3-measurements. The IWV values derived from GPS ZPD measurements exhibited high relative scatter for low IWV (smaller than 10×10^{21} mol/cm^2). For lowest IWV (smaller than 5×10^{21} mol/cm^2), they were even inferior to the RAM data. This means that the gap during night time, cloudy weather conditions, and in the polar winter can however be filled using the GPS, except for very low IWV. Similar conclusions can be drawn for the satellite-based instruments SCIAMACHY, GOME,

and AMSU-B. The strength of the GOME and the SCIAMACHY is the ability to measure high IWV but rely on solar irradiation of the atmosphere and on little interference by clouds. AMSU-B, however, does not rely on external irradiation of the atmosphere and delivers data throughout polar winter.

Thus, our analysis shows that, despite efforts to develop various methods and tools for monitoring the concentration of water vapor in the atmosphere, our possibilities for measuring the complete seasonal cycle are still very limited (Palm et al. 2010). The typical surface station instruments commonly provide only very local, point, observations, and therefore suffer from low spatial resolution. Compounding this problem is the limited accessibility to position humidity gauges in heterogeneous terrain, or areas with complex topography. In addition, because of surface perturbation a point measurement close to the surface (e.g., 2 m from the ground as in a standard meteorological surface station) is not satisfactory for model initialization. What is ideally required for meteorological modeling purposes is an area average measurement of near-surface moisture over a box with the scale of the model's grid and at an altitude of a few tens of meters. Sensors installed on both commercial and research aircraft to measure water vapor also can be used for *in situ* atmosphere monitoring. Of course, this approach to humidity measurement is a promising. However, this approach would only provide measurements when and where scheduled flights occur and thus the researcher might not have data where they are needed. In addition, the cost is high for dedicated aircraft flights. Another approach is to fly small *in situ* packages on balloons filled with helium or hydrogen. However, radiosondes, which are typically launched only 2–4 times a day, also provide very limited information. In addition, these monitoring methods are costly for implementation, deployment, and maintenance. In addition, it was established that data from radiosondes have biases that lead to underestimation of relative humidity, particularly in the mid and UT (e.g., Soden et al. 1994; Ferrare et al. 1995; Lesht and Liljegren 1997; Kley et al. 2000; Miloshevich et al. 2001; Wang et al. 2002; Turner et al. 2003; Soden et al. 2004). Wang et al. (2002) identified the source of some of the biases, including contamination of the sensor due to inappropriate packaging of the radiosondes prior to use, errors in the model relating the change of capacitance of the humidity sensor with changes in relative humidity, and errors in the model relating the change of capacitance of the humidity sensor with changes in temperature. Soden et al. (2004) applied the bias corrections of Wang et al. (2002) and found that upper-tropospheric humidity is still underestimated (up to 40%) by radiosondes compared with LIDAR and IR satellite measurements, which means the cause (or causes) of the radiosonde dry bias is (or are) still largely unknown. In recent years, much attention has been paid to the use of satellites for these purposes. Satellites allow for a large area to be covered, but results obtained by satellites are frequently not accurate enough in measuring surface-level moisture, whereas this near-surface moisture is, in most cases, the important variable for convection. In addition, the application of satellites for these purposes is possible primarily for only cloud-free zones. Microwave sounders have the ability to sound through cloud and hence offer nearly all-weather capability. However, their spatial resolution (both vertical and horizontal) is generally lower than that of the IR instruments. So, further research aimed at finding and developing new methods of monitoring the atmosphere is still required.

REFERENCES

Anderson J.G., Wilmouth D.M., Smith J.B., Sayres D.S. (2012) UV dosage levels in summer: Increased risk of ozone loss from convectively injected water vapor. *Science* 337, 835–839.

Bange J., Espositi M., Lenschow D.H. et al. (2013) Measurement of aircraft state and thermodynamic and dynamic variables. In: Wendisch M., Brenguier J.-L. (Eds.), *Airborne Measurements for Environmental Research. Methods and Instruments.* Wiley-VCH, Weinheim, Germany, Chapter 2.

Beaton S.P., Spowart M. (2012) UV absorption hygrometer for fast–response airborne water vapor measurements. *J. Atmos. Oceanic. Technol.* 29, 1295–1303.

Bertaux J.-L., Delannoy A. (1978) Vertical distribution of H_2O in the stratosphere as determined by UV fluorescence in-situ measurements. *Geophys. Res. Lett.* 5, 1017–1020.

Buck A.L. (1976) The variable–path Lyman–alpha hygrometer and its operating characteristics. *Bull. Amer. Meteor. Soc.* 57, 1113–1118.

Buck A.L. (1985) The Lyman-alpha absorption hygrometer. In: *Proceedings, Moisture and Humidity Symposium*, Washington, DC, Instrument Society of America, Research Triangle Park, NC, p. 411.

Buehler S.A., Kuvatov M., John V.O., Milz M., Soden B.J., Jackson D.L., Notholt J. (2008), An upper tropospheric humidity data set from operational satellite microwave data. *J. Geophys. Res.* 113, D14110.

Campbell G.S., Tanner B.D. (1985) A krypton hygrometer for measurement of atmospheric water vapor concentration. In: Moisture and Humidity: Measurement and Control in Science and Industry. Instrument Society of America, Research Triangle Park, *Proceedings of the 1985 International Symposium on Moisture and Humidity*, Instrument Society of America, pp. 609–614.

Chou C., Neelin J.D., Chen C.A., Tu J.Y. (2009) Evaluating the "rich-get-richer" mechanism in tropical precipitation change under global warming. *J. Clim.* 22, 1982–2005.

De F. Forster P.M., Shine K.P. (1999) Stratospheric water vapour changes as a possible contributor to observed stratospheric cooling. *Geophys. Res. Lett.* 26, 3309–3312.

Dessler A.E., Sherwood S.C. (2004) Effect of convection on the summertime extratropical lower stratosphere. *J. Geophys. Res.* 109, D23301.

Engelen R.J., Stephens G.L. (1999) Characterization of water-vapour retrievals from TOVS/HIRS and SSM/T-2 measurements. *Q. J. Royal Meteorol. Soc.* 125, 331–351.

Ferrare R.A., Melfi S.H., Whiteman D.N., Evans K.D., Schmidlin F.J., O'C Starr D. (1995) A comparison of water vapor measurements made by Raman Lidar and radiosondes. *J. Atmos. Ocean. Technol.* 12, 1177–1195.

Fetzer E.J., Read W.R., Waliser D. et al. (2008) Comparison of upper tropospheric water vapor observations from the microwave limb sounder and atmospheric infrared sounder. *J. Geophys. Res.* 113, D22110.

Froidevaux L., Livesey N.J., Read W.G. et al. (2006), Early validation analyses of atmospheric profiles from EOS MLS on the Aura satellite. *IEEE Trans. Geosci. Remote Sens.* 44, 1106–1121.

Goutail F., Pommereau J.-P. (1987) Stratospheric water vapor in situ measurements from infra-red montgolfier. *Adv. Space Res.* 7(7), 111–114.

Hall P., Dumas E., Senn D. (2006) NOAA ARL mobile flux platform instrumentation integration on University of Alabama Sky Arrow Environmental Aircraft. NOAA Technical Memorandum, ARL-257, 51 p.

Harries J.E. (1997) Atmospheric radiation and atmospheric humidity. *Q. J. Royal Meteorol. Soc.* 123, 2173–2186.

Hintsa E.J., Weinstock E.M., Anderson J.G., May R.D., Hurst D. (1999) On the accuracy of *in situ* water vapor measurements in the troposphere and lower stratosphere with the Harvard Lyman-α hygrometer. *J. Geophys. Res.* 104, 8183–8189.

Hurst D.F., Oltmans S.J., Vömel H., Rosenlof K.H., Davis S.M., Ray E.A., Hall E.G., Jordan A.F. (2011) Stratospheric water vapor trends over Boulder, Colorado: Analysis of the 30 year Boulder record. *J. Geophys. Res.* 116, D02306.

Hurst D.F., Lambert A., Read W.G., Davis S.M., Rosenlof K.H., Hall E.G., Jordan A.F., Oltmans S.J. (2014) Validation of Aura microwave limb sounder stratospheric water vapor measurement by the NOAA frost point hygrometer. *J. Geophys. Res. Atmos.* 119, 1612–1625.

IPCC (2007) Climate Change 2007. Fourth assessment report: Synthesis report. http://www.ipcc.ch/publications_and_data/ar4/syr/en/contents.html.

Kaufmann S., Voigt C., Jurkat T., Thornberry T., Fahey D.W., Gao R.-S., Schlage R., Schäuble D., Zöger M. (2016) The airborne mass spectrometer AIMS—Part 1: AIMS-H_2O for UTLS water vapor measurements. *Atmos. Meas. Tech.* 9, 939–953.

Kebabian P., Kolb C.E., Freedman A. (2002) Spectroscopic water vapor sensor for rapid response measurements of humidity in the troposphere. *J. Geophys. Res. Atmos.* 107(23), 4670.

Kirk-Davidoff D.B., Hintsa E.J., Anderson J.G., Keith D.W. (1999) The effect of climate change on ozone depletion through changes in stratospheric water vapour. *Nature* 402(6760), 399–401.

Kley D., Stone E. (1978) Measurements of water vapor in the stratosphere by photo dissociation with Ly-α (1216 Å) light. *Rev. Sci. Instrum.* 49(6), 691–697.

Kley D., Stone E.J., Henderson W.R., Drummond J.W., Harrop W.J., Schmeltekopf A.L., Thompson T.L., Winkler R.H. (1979) *In situ* measurements of the mixing ratio of water vapor in the stratosphere, *J. Atmos. Sci.* 36, 2513–2524.

Kley D., Russell J.M. III, Phillips C. (Eds.) (2000) SPARC assessment of upper tropospheric and stratospheric water vapor. World Meteorological Organization Technical Document 143. SPARC Report No.2. World Climate Research Programme, Geneva, Switzerland.

Leblanc T., McDermid I.S., Walsh T.D. (2012) Ground-based water vapor Raman lidar measurements up to the upper troposphere and lower stratosphere for long-term monitoring. *Atmos. Meas. Tech.* 5, 17–36.

Lesht B.M., Liljegren J.C. (1997) Comparison of precipitable water vapor measurements obtained by microwave radiometers and radiosondes at the southern great plains cloud and radiation Testbed Site. In: *Proceedings of the Sixth Atmospheric Radiation Measurement Science Team Meeting*, San Antonio, TX, pp. 165–168.

Mastenbrook H.J. (1968) Water vapor distribution in the stratosphere and high troposphere. *J. Atmos. Sci.* 25, 299–311.

May R.D. (1998) Open–path, near–infrared tunable diode laser spectrometer for atmospheric measurements of H_2O. *J. Geophys. Res.* 103(D15), 19161–19172.

Menzel W.P., Purdom J.F.W. (1994) Introducing *GOES-I:* The first of a new generation of geostationary operational environmental satellites. *Bull. Am. Meteo. Soc.* 75, 757–781.

Miloshevich L.M., Vomel H., Paukkunen A., Heymsfield A.J., Oltmans S.J. (2001) Characterization and correction of relative humidity measurements from Vaisala RS80A radiosondes at cold temperatures. *J. Atmos. Oceanic Technol.* 18, 135–155.

Noël S., Buchwitz M., Bovensmann H., Hoogen R., Burrows J.P. (1999) Atmospheric water vapor amounts retrieved from GOME satellite data. *Geophys. Res. Lett.* 26(13), 1841–1844.

Oltmans S.J., Hofmann D.J. (1995) Increase in lower-stratospheric water vapor at a mid-latitude Northern Hemisphere site from 1981 to 1994. *Nature* 374, 146–149.

Palm M., Melsheimer C., Noel S., Heise S., Notholt J., Burrows J., Schrems O. (2010) Integrated water vapor above Ny Alesund, Spitsbergen: A multi-sensor intercomparison. *Atmos. Chem. Phys.* 10, 1215–1226.

Pankine A., Nock K., Li Z., Parsons D., Purucker M., Wiscombe W., Weinstock E. (2009) Stratospheric satellites for earth observations. *BAMS* 97(8), 1109–1119.

Rind D., Lonergan P. (1995) Modeled impacts of stratospheric ozone and water vapour perturbations with implications for high speed civil transport aircraft. *J. Geophys. Res.* 1007381–1007396.

Schanot A.J. (1987) An evaluation of the uses and limitations of Lyman-alpha hygrometer as an operational airborne humidity sensor. In: *Proceedings of 6th Symposium Meteorological Observations and Instrumentation*, New Orleans, LA., American Meteorological Society, pp. 257–260.

Schmetz J., Pili P., Tjemkes S., Just D., Kerkmann J., Rota S., Ratier A. (2002) An introduction to Meteosat second generation (MSG). *Bull. Am. Meteorol. Soc.* 83, 977–992.

Schneider M., Romero P.M., Hase F., Blumenstock T., Cuevas E., Ramos R. (2009) Quality assessment of Izana's upper-air water vapour measurement techniques: FTIR, Cimel, MFRSR, GPS, and Vaisala RS92. *Atmos. Meas. Tech. Discuss.* 2, 1625–1662.

Schneider M., Toon G.C., Blavier J.-F., Hase F., Leblanc T. (2010a) H_2O and D profiles remotely-sensed from ground in different spectral infrared regions. *Atmos. Meas. Tech.* 3:1599–1613.

Schneider M., Romero P.M., Hase F., Blumenstock T., Cuevas E., Ramos R. (2010b) Continuous quality assessment of atmospheric water vapour measurement techniques: FTIR, Cimel, MFRSR, GPS, and Vaisala RS92. *Atmos. Meas. Tech.* 3, 323–338.

Schneider M., Demoulin P., Sussmann R., Notholt J. (2013) Fourier transform infrared spectrometry. In: Kampfer, N. (Ed.), *Monitoring Atmospheric Water Vapor*. Springer, New York, pp. 95–112.

Shannon C.E. (1949) Communication in the presence of noise. *Proc. Inst. Radio Eng.* 37, 10–21.

Sherwood S.C., Roca R., Weckwerth T.M., Andronova N.G. (2010) Tropospheric water vapor, convection, and climate. *Rev. Geophys.* 48, RG2001.

Soden B.J., Ackerman S.A., O'C Starr D., Melfi S.H., Ferrare R.A. (1994) Comparison of upper tropospheric water vapor from GOES, Raman lidar, and CLASS sonde measurements. *J. Geoph. Res.* 99, 21005–21016.

Soden B.J., Turner D.D., Lesht B.M., Miloshevich L.M. (2004) An analysis of satellite, radiosonde, and lidar observations of upper tropospheric water vapor from the ARM program. *J. Geoph. Res.* 109, D04105.

Solomon S., Rosenlof K.H., Portmann R.W., Daniel J.S., Davis S.M., Sanford T.J., Plattner G.K. (2010) Contributions of stratospheric water vapor to decadal changes in the rate of global warming. *Science* 327(5970), 1219–1223.

Susskind J., Barnet C.D., Blaisdell J.M. (2003) Retrieval of atmospheric and surface parameters from AIRS/AMSU/HSB data in the presence of clouds. *IEEE Trans. Geosci. Remote Sens.* 41, 390–409.

Tillman J.E. (1965) Water vapor density measurements utilizing the absorption of vacuum ultraviolet and infrared radiation. In: Ruskin R.E. (Ed.), *Humidity and Moisture*, Vol. 1, Principles and Methods of Measuring Humidity in Gases. Reinhold, Wisconsin, WI, pp. 428–443.

Trapp R.J., Diffenbaugh N.S., Gluhovsky A. (2009) Transient response of severe thunderstorm forcing to elevated greenhouse gas concentrations. *Geophys. Res. Lett.* 36, L01703.

Turner D.D., Lesht B.M., Clough S.A., Liljegren J.C., Revercomb H.E., Tobin D.C. (2003) Dry bias and variability in Vaisala radiosondes: The ARM experience. *J. Atmos. Oceanic Technol.* 20, 117–132.

Van Klooster S.L., Roebber P.J. (2009), Surface-based convective potential in the contiguous United States in a business-as-usual future climate. *J. Climate* 22, 3317–3330.

Vömel H., Yushkov V., Khaykin S., Korshunov L., Kyro E., Kivi R. (2007) Intercomparison of stratospheric water vapor sensors: FLASH-B and NOAA/CMDL frost point hygrometer. *J. Atmos. Oceanic Tech.* 27, 941–952.

Wang J.H., Zhang L.Y. (2008) Systematic errors in global radiosonde precipitable water data from comparisons with ground-based GPS measurements. *J. Clim.* 21, 2218–2238.

Wang J., Cole H.L., Carlson D.J., Miller E.R., Beirle K., Paukkunen A., Laine T.K. (2002) Corrections of humidity measurement errors from the Vaisala RS80 radiosonde—application to TOGA-COARE data. *J. Atmos. Oceanic Technol.* 19, 981–1002.

Waters J.W., Froidevaux L., Harwood R.S., Jarnot R.F., Pickett H.M., Read W.G. et al. (2006) The Earth observing system microwave limb sounder (EOS-MLS) on the Aura satellite. *IEEE Trans. Geosci. Remote Sens.* 44, 1075–1092.

Weinheimer A.J., Schwiesow R.L. (1992) A two–path, two–wavelength ultraviolet hygrometer. *J. Atmos. Oceanic Technol.* 9, 407–419.

Yoshino K., Esmond J.R., Parkinson W.H., Ito K., Matsui T. (1996) Absorption cross section measurements of water vapor in the wavelength region 120 to 188 nm. *Chem. Phys.* 211, 387–391.

Zondlo M.A., Paige M.E., Massick S.M., Silver J.A. (2010) Vertical cavity laser hygrometer for the National Science Foundation Gulfstream-V aircraft. *J. Geophys. Res.* 115, D20309.

Zuber A., Witt G. (1987) Optical hygrometer using differential absorption of hydrogen Lyman–α radiation. *Appl. Opt.* 26(15) 3083–3089.